J|A|C|S
ARTICLES
Published on Web 12/14/2005

Reagentless, Reusable, Ultrasensitive Electrochemical Molecular Beacon Aptasensor

Abd-Elgawad Radi,*[,†,‡] Josep Lluis Acero Sánchez,[‡] Eva Baldrich,[‡] and Ciara K. O'Sullivan*[,‡,§]

Contribution from the Nanobiotechnology and Bioanalysis Group, Department of Chemical Engineering, Universitat Rovira i Virgili, Tarragona, Spain, and Institució Catalana de Recerca i Estudis Avançats, Passeig Lluís Company 23, 08010 Barcelona, Spain, and Department of Chemistry, Faculty of Science, Mansoura University, 34517 Dumyat, Egypt

Received May 12, 2005; E-mail: ciara.osullivan@urv.net; abd.radi@urv.net

Abstract: A bifunctional derivative of the thrombin-binding aptamer with a redox-active Fc moiety and a thiol group at the termini of the aptamer strand was synthesized. The ferrocene-labeled aptamer thiol was self-assembled through S−Au bonding on a polycrystalline gold electrode surface and the surface was blocked with 2-mercaptoethanol to form a mixed monolayer. By use of a fluorescent molecular beacon, the effect of counterions on quadruplex formation was established. The aptamer-modified electrode was characterized electrochemically by cyclic voltammetry (CV), differential pulse voltammetry (DPV), and electrochemical impedance spectroscopy (EIS). The modified electrode showed a voltammetric signal due to a one-step redox reaction of the surface-confined ferrocenyl moiety of the aptamer immobilized on the electrode surface in 10 mM *N*-(2-hydroxyethyl)piperazine-*N*′-2-ethanesulfonic acid (HEPES) buffer of pH 8.0. An increase in the DPV current signal was evident after blocking with 2-mercaptoethanol, effectively removing aptamer nonspecifically absorbed rather than bound to electrode surface or due to the formation of the aptamer−thrombin affinity interaction. The impedance measurement, in agreement with the differential pulse voltammetry (DPV), showed decreased Faradaic resistances in the same sequence. The "signal-on" upon thrombin association could be attributed to a change in conformation from random coil-like configuration on the probe-modified film to the quadruplex structure. The DPV of the modified electrode showed a linear response of the Fc oxidation signal to the increase in the thrombin concentration in the range between 5.0 and 35.0 nM with a linear correlation of $r = 0.9988$ and a detection limit of 0.5 nM. The molecular beacon aptasensor was amenable to full regeneration by simply unfolding the aptamer in 1.0 M HCl, and could be regenerated 25 times with no loss in electrochemical signal upon subsequent thrombin binding.

1. Introduction

Affinity biosensors have garnered much attention over the last two decades due to their wide potential applicability in clinical, environmental, and food analysis. Despite concerted efforts, few reports have been made of affinity sensors that fulfill the desired requirements of being reagentless, reusable, and ultrasensitive, with the only required end-user intervention being the addition of sample.

Electrochemical methods have received particular attention due to their high sensitivity and selectivity, simple instrumentation, low production cost, and the fact that they are fast, accurate, compact, portable, and inexpensive. Many of the electrochemical strategies are based on a change in the electrochemical response of an electroactive label bound to bioorganic molecules probes. In this context, ferrocene as a label has been the subject of intense investigation, as it is a molecule that exhibits excellent reversibility of its redox reaction and offers the versatility of synthesizing various Fc derivatives.[1] The electrochemistry of ferrocene derivatives and their potential application for the development of Fc-based electrochemical biosensors is presently receiving a significant amount of attention.[2−9] Research into Fc-based DNA biosensor has been particularly successful, providing new methods for detection of DNA hybridization, mutations, DNA lesions, gene sequencing, and DNA/protein interaction.[10−13]

† Mansoura University.
‡ Universitat Rovira i Virgili.
§ ICREA.

(1) Van Staveren, D. R.; Metzler-Nolte, N. *Chem. Rev.* **2004**, *10*, 5931−5986.
(2) Bu, H.; English, A. M.; Mikkelsen, S. R. *Anal. Chem.* **1996**, *68*, 3951−3957.
(3) Smalley, J. F.; Sachs, S. B.; Chidsey, C. E. D.; Dudek, S. P.; Sikes, H. D.; Creager, S. E.; Yu, C. J.; Feldberg, S. W.; Newton, M. D. *J. Am. Chem. Soc.* **2004**, *126*, 14620−14630.
(4) Forrow, N. J.; Foulds, N. C.; Frew, J. E.; Law, J. T. *Bioconjugate Chem.* **2004**, *15*, 137−144.
(5) Bu, H.-Z.; Mikkelsen, S. R.; English, A. M. *Anal. Chem.* **1998**, *70*, 4320−4325.
(6) Schuhmann, W. *Biosens. Bioelectron.* **1995**, *10*, 181−193.
(7) Oungpipat, W.; Alexander P. W.; Southwell-Keely, P. *Anal. Chim. Acta* **1995**, *309* (20), 35−45.
(8) Okawa, Y.; Nagano, M.; Hirota, S.; Kobayashi, H.; Ohno, T.; Watanabe, M. *Biosens. Bioelectron.* **1999**, *14*, 229−235.
(9) Yu, C. J.; Wan, Y.; Yowanto, H.; Li, J.; Tao, C.; James, M. D.; Tan, C. L.; Blackburn, G. F.; Meade, T. J. *J. Am. Chem. Soc.* **2001**, *123*, 11155−11161.
(10) Patolsky, F.; Weizmann, Y.; Willner, I. *J. Am. Chem. Soc.* **2002**, *124*, 770−772.

Aptamers, reported for the first time in 1990,[14−16] are oligonucleotides selected from combinatorial libraries by SELEX, systematic evolution of ligands by exponential enrichment. Aptamers against a variety of targets have been produced,[17−22] often showing affinity and specificity equaling or even surpassing those of antibodies. Their unique chemical characteristics and method of production presents aptamers as excellent biorecognition elements. Aptamers possess significant advantages over other recognition molecules, such as antibodies, such as their small size, chemical simplicity, and flexibility. In addition, aptamers can be easily modified to incorporate molecular markers or to favor immobilization, can be produced and used under nonphysiological conditions, and can be reversibly denatured, allowing the optimization of reusable devices[23−25] such as molecular beacons.

The first fluorescent molecular beacon (MB) was initially described in 1996 as nucleic acid probe able to undergo spontaneous conformational change following hybridization with the complementary nucleic acid target.[26] Such a conformational change was translated into either a quenching or a change in fluorescence emission by inducing physical separation of a fluorophore/quenching pair (in the quenching formats) or a pair or donor/acceptor fluorophores (in the FRET formats). An electrochemical approximation has also been reported by incorporating an electroactive tag to a DNA probe immobilized on a gold electrode[27,28] and using cyclic voltammetry to measure the changes in electron transfer induced by hybridization.

Here, we report the development of an electrochemical molecular aptamer beacon that combines the significant advantages of the electrochemical detection of a rapid and real-time monitoring of the biorecognition event with the versatility of reagentless, reusable, surface-attached molecular beacons. This employs a bifunctionalized aptamer with a terminal electroactive ferrocene group as the reporter and the thiol function as the anchor on a gold electrode surface. The immobilized ferrocene-labeled aptamer showed a voltammetric signal due to a one-step redox reaction of the ferrocenyl moiety. In a recent paper, an analogous route in which the signal is switched "off" was reported.[29] In our approach, an enhanced electrochemical signal is generated upon recognition of the target protein (i.e., signal "on" device). In this recent report,[29] a 32-base thrombin-binding DNA aptamer labeled with methylene blue (MB) was used. In the absence of thrombin, the aptamer is thought to remain relatively unfolded, thereby allowing the attached MB to collide with the electrode and transfer an electron. Upon thrombin binding, electron transfer is inhibited, presumably due to a binding-induced conformational change in the aptamer that significantly increases the electron-tunneling distance. In the present study reported here, the 15-base aptamer used also undergoes a conformational equilibrium between its unfolded state and the folded quadruplex structure. However, due to the short aptamer length, this conformational change resulting in the folded quadruplex structure due to target binding, significantly decreases electron-tunneling distance, bringing the ferrocene label to the electrode surface and thus, enhancing the electron transfer.

2. Experimental Section

2.1. Materials and Methods. The variants of the thrombin-binding aptamer (TBA, 5′-GGTTGGTGTGGTTGG-3′), HPLC-purified and lyophilized, were provided by Molecular Solutions (London). TBA, 3′-biotinylated through a hexamethylene linker, was used for the study of regeneration agents by an enzyme-linked aptamer assay (ELAA). A fluorescent molecular beacon, with 6-FAM (FAM = carboxyfluorescein) (with a 3-carbon spacer) at the 5′ end and coumarin (with a 6-carbon spacer) at the 3′ end, was used to study the effect of different counterions on the TBA structure. TBA modified with -SH at the 3′ end and -NH at the 5′ end (SH-TBA-NH_2), both incorporated through 6-carbon spacers, was used to produce an electrochemical molecular beacon.

Pure human thrombin was supplied by Haematologic Technologies Inc.(Essex Junction, VT It was chemically conjugated to horseradish peroxidase (Sigma, Barcelona, Spain) by the SATA/sulfo-SMCC method described in ref 30. Immunoglobulin G (IgG) bovine serum albumin (BSA) and streptavidin were provided by Sigma (Barcelona Spain).

2.2. Synthesis of Ferrocene-Labeled Electrochemical Molecular Beacon. The electrochemical molecular beacon was produced by incorporation of a ferrocene label to the 5′-ter of the SH-TBA-NH by the EDC−NHS method. Briefly, 10 nmol of DNA (50 μg) was incubated for 2 h in 100 μL of 10 mM phosphate-buffered saline (PBS), pH 7.4 containing 20 nmol of ferrocenecarboxylic acid, 1 mM 1-ethyl-3-[(3-dimethylamino)propyl]carbodiimide (EDC), and 5 mM *N*-hydroxysuccinimide (NHS), provided by Sigma (Barcelona, Spain). The conjugate was desalted on a G-25 column (Amersham-Pharmacia; Barcelona, Spain) and its concentration was evaluated by UV−vis spectrophotometry. Subtraction of the A_{260} due to the ferrocene label was attempted by characterizing the A_{260} and A_{450} of a dilution series of the ferrocenecarboxylic acid.

2.3. Electrochemical Measurements. All electrochemical measurements were performed with a potentiostat/galvanostal PGSTAT 30 Autolab (Ecochemie, Utrecht, The Netherlands) in a one-compartment cell with a three-electrode system consisting of a modified gold working electrode, an Ag−AgCl reference electrode, and a platinum counter-electrode in 5 mL of 0.1 M *N*-(2-hydroxyethyl)piperazine-*N*′-2-ethanesulfonic acid (HEPES) buffer (pH 8.0). Differential pulse voltammograms (DPVs) were registered in the potential interval −0.2 to +0.5 V vs Ag−AgCl, under the following conditions: modulation amplitude 0.05 V, step potential 0.001 V, and scan rate 0.002 V s^{-1}.

Electrochemical impedance experiments were performed at the formal potential of attached ferrocene ($E°$ = 0.165 V vs Ag−AgCl

(11) Wang, J.; Li, J.; Baca, A. J.; Hu, J.; Zhou, F.; Yan, W.; Pang, D.-W. *Anal. Chem.* **2003**, *75*, 3941−3945.
(12) Liu, J.; Tian, S.; Tiefenauer, L.; Nielsen, P. E.; Knoll, W. *Anal. Chem.* **2005**, *77*, 2756−2761.
(13) Georgopoulou, A. S.; Mingos, D. M. P.; White, A. J. P.; Williams, D. J.; Horrocks, B. R.; Houlton, A. *J. Chem. Soc., Dalton Trans.* **2000**, 2969−2974.
(14) Robertson, D. L.; Joyce, G. F. *Nature* **1990**, *344*, 467−468.
(15) Ellington, A. D.; Szostak, J. W. *Nature* **1990**, *346*, 818−822.
(16) Tuerk, C.; Gold, L. *Science* **1990**, *249*, 505−510.
(17) Hesselberth, J.; Robertson, M. P.; Jhaveri, S.; Ellington, A. D. *Mol. Biotechnol.* **2000**, *74*, 15−25.
(18) Haller, A. A.; Sarnow, P. *Proc. Natl. Acad. Sci. U.S.A.* **1997**, *94*, 8521−8526.
(19) Gebhardt, K.; Shokraei, A.; Babaie, E.; Lindquist, B. H. *Biochem.* **2000**, *39*, 7255−7265.
(20) Bruno, J. G.; Kiel, J. L. *Biosens. Bioelectron.* **1999**, 31 (*14*), 457−464.
(21) Wilson, D. S.; Keefe, A. D.; Szostak, J. W. *Proc. Natl. Acad. Sci. U.S.A.* **2001**, *98*, 3750−3755.
(22) Kawakami, J.; Imanaka, H.; Yokota, Y.; Sugimoto, N. *J. Inorg. Biochem.* **2000**, *82*, 197−206.
(23) Bruno, J. G.; Kiel, J. L. *BioTechniques* **2002**, *32*, 178−183.
(24) Murphy, M. B.; Fuller, S. T.; Richardson P. M.; Doyle, S. A. *Nucleic Acids Res.* **2003**, *31*, e110.
(25) Asai, R.; Nishimura, S. I.; Aita, T.; Takahashi, K. *Anal. Lett.* **2004**, *37*, 645−656.
(26) Tyagi, S.; Kramer, F. R. *Nat. Biotechnol.* **1996**, *14*, 303−308.
(27) Fan, C.; Plaxco, K. W.; Heeger, A. J. *Proc. Natl. Acad. Sci. U.S.A.* **2003**, *100* (16), 9134−9137.
(28) Mao, Y.; Luo, C.; Ouyang, Q. *Nucleic Acids Res.* **2003**, *31* (18), e108.
(29) Xiao, Y.; Lubin, A. A.; Heeger, A. J.; Plaxco, K. W. *Angew. Chem., Int. Ed.* **2005**, *44*, 5456−5459.
(30) Hermanson, G. T. *Bioconjugate Technique*; Academic Press: San Diego, CA, 1996.

and an alternating potential ac with amplitude of 5 mV at the frequency range from 100 kHz to 10 mHz. A Nyquist plot (Z_{re} vs Z_{im}) was drawn to analyze the impedance results.

2.4. Effect of Counterions. The effects induced by different counterions on the TBA conformation were studied by use of a fluorescent molecular beacon (MB). Aliquots (100 μL) of the fluorescent MB, diluted to 250 nM in HEPES buffer, were placed in each well of a microtiter plate. Fluorescent emission was measured before and after the addition of a dilution series of KCl, NaCl, $MgCl_2$, or LiCl (10 μL/well, final concentrations 0.78 mM−2 M). The effect of such ions on the formation of the aptamer quadruplex was analyzed by measuring the MB fluorescence with/without each salt, before and after addition of a dilution series of thrombin.

2.5. Probe Immobilization Procedure. Electrodes were cleaned by exposure to warm piranha solution for 1 h. [Piranha solution is a 1:3 (v/v) mixture of 30% H_2O_2 and concentrated H_2SO_4. *Warning: This solution reacts violently with organic materials and should be handled with great care.*] The cleaned gold electrode was held upside down, covered with a plastic cap, and 50 μL of 0.5 μM Fc-TBA-SH in 1.0 M KH_2PO_4 buffer solution was dropped onto the electrode surface. The electrode was then covered with 50 μL of 1.0 M KH_2PO_4 buffer solution containing 0.1 M 2-mercaptoethanol (2-ME) solution for 10 min. Subsequently; the electrodes were placed in 1.0 M HCl, under stirring conditions, for 10 min and rinsed thoroughly with a copious amount of deionized water. This eliminated the presence of any trace counterions that may have been present in the buffers used in the immobilization and blocking procedure. For each assay, 50 μL of 10 mM HEPES buffer solution containing a given concentration of the target thrombin was dropped onto the electrode covered with the aptamer/2-ME mixed self-assembled monolayer (SAM), and the reaction was allowed to proceed for 10 min. After the surface was thoroughly rinsed with a washing buffer, the electrode was mounted into an electrochemical cell. Prior to storage, the electrodes were rinsed thoroughly with deionized water and dried under a stream of nitrogen. The whole procedure was performed at room temperature.

2.6. Regeneration of Electrochemical Molecular Aptamer Beacon. The efficiency of different regenerating agents was studied by ELAA as follows. The 3′-biotinylated TBA (100 μL/well, 50 nM diluted in PBS) was immobilized on streptavidin-coated plates (kindly supplied by CanAg Diagnostics, Gothenburg, Sweden) for 30 min at 37 °C and then washed thoroughly prior to addition of thrombin-HRP (23 nM), for 60 min at 4 °C. The plates were again thoroughly washed and the presence of enzyme label was optically detected. Following washing, different regenerating agents (100 μL/well) were applied to the plate for 10 min at room temperature. Two different concentrations of the following regenerating agents were tested: HCl (1 and 0.01 M), SDS (10% and 2%), Na_2CO_3 (0.2 and 0.05 M), NaCl (2 and 0.1 M), NaOH (1 and 0.05 M), LiCl (1 and 0.01 M), and glycine (2 and 0.01 M). After washing, TMB (50 μL/well) was added into the wells and the presence of enzyme label was again optically detected. This entire process of capture and regeneration was repeated, and all experiments were carried out in triplicate.

Different controls were carried out to check the performance of this system. Control 1 consisted of the addition of each regenerating agent (100 μL/well) for 10 min at room temperature before the addition of the biotinylated TBA. Then a direct capture assay was performed as it is described above. This control was used to check the effect of the regenerating agents on the streptavidin-coated plates. Control 2 was carried out to check the nonspecific adsorption of the HRP-labeled thrombin on the streptavidin-coated plate previously treated with the regenerating agent. Hence, each regenerating agent (100 μL/well) was applied to the plate for 10 min at room temperature. Following washing, a 23 nM solution (50 μL/well) of thrombin-HRP was added into the wells for 1 h at 4 °C. Finally, control 3 consisted of the mixing of the HRP-labeled thrombin with each regenerating agent for 10 min at room temperature.

The best candidate for regeneration (1.0 M HCl) was further evaluated by DPV, exposing the aptamer-modified electrode to repeated cycles of regeneration and capture.

3. Results and Discussion

3.1. Study of the Effect of Different Counterions on the TBA Conformation. A routine regeneration protocol when working with aptamers consists of the addition of high concentrations of salt (often 2 M NaCl or KCl), which causes disruption of the hydrogen bonds and electrostatic interactions responsible for most of the aptamer−target association. In addition, it is known that, for the optimal performance of electrochemical detection methods, the presence of counterions in the medium is desirable. However, it has been demonstrated that the presence of certain ions can induce the folding of some aptamers in a manner similar to their molecular targets, as is in fact the case with TBA in the presence of KCl.[31] This fact is of crucial importance in the optimization of assay formats whose sensitivity depends on signal transduction associated with the conformational rearrangement induced by target binding, such as molecular beacons. In the context of the work reported here, folding of the TBA electrochemical MB due to the presence of specific ions would induce physical approximation of the electrochemical tag to the electrode surface, and thus signal increase, even in the absence of thrombin.

For this reason, the effect of different counterions on the TBA folding was evaluated by use of a TBA fluorescent MB (TBA-FMB), containing FAM at one extreme and coumarin at the other. It had been previously observed that the incubation of the TBA-FMB in the presence/absence of different concentrations of either thrombin or KCl correlated with structural rearrangement/tightening, and thus fluorescence quenching.[31] This was presumably due to the proximity of the fluorophores to each other, as well as to their proximity to the TBA G-8, guanines having a well-known quenching effect on fluorophores. In an effort to find counterions that could be used for electrochemical work, the effect of other monovalent ions, including NaCl and LiCl as well as $MgCl_2$, has also been studied (Figure 1a).

The addition of 0.78−100 mM $MgCl_2$ to the TBA-FMB in solution induced a consistent decrease in fluorescent emission of the MB. This salt was thus avoided in future experiments. The addition of KCl resulted in a quenching proportional to its concentration. However, the addition of 0.78−100 mM either NaCl or LiCl had no effect on the beacon fluorescence.

Our previous experiments had demonstrated that the presence of KCl decreased the TBA-FMB sensitivity when thrombin was detected in solution. In this study, the effect of thrombin addition on the FMB emission was studied in the presence/absence of 25 mM KCl, NaCl, LiCl, or $MgCl_2$. The best results were always obtained in the absence of stabilizing salts (experiment carried out in just HEPES). While such concentrations of NaCl or LiCl had little effect on thrombin detectability with the MB, KCl induced an important decrease in the quenching level (Figure 1b).

3.2. Cyclic Voltammetry. Figure 2 shows the cyclic voltammogram of a gold electrode modified by the ferrocenyl aptamer thiol monolayer in blank HEPES buffer solution (0.0 M, pH 8.0) at a sweep rate of 100 mV s^{-1}. A quasi-reversible

(31) Baldrich, E.; O'Sullivan C. K. *Anal. Biochem.* **2005**, *341*, 194−197.

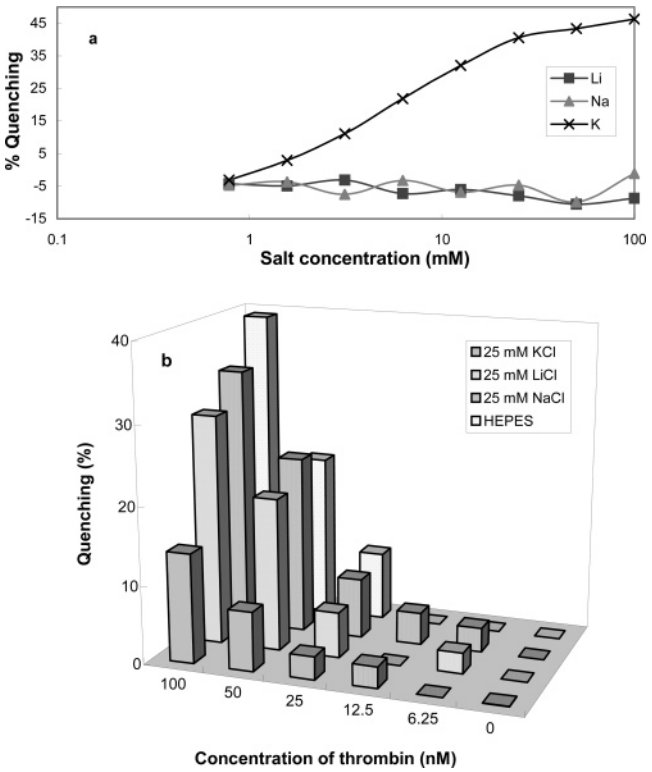

Figure 1. Effect of the presence of salt on the performance of TBA molecular beacons. (a) Effect of the presence of different concentrations of KCl, NaCl, or LiCl on the TBA fluorescent molecular beacon. (b) Thrombin detectability of the TBA fluorescent molecular beacon in the presence and in the absence of different salts.

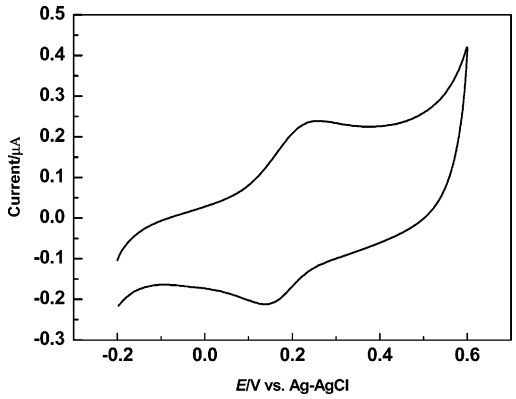

Figure 2. Cyclic voltammograms of Fc-TBA-coated Au electrode in blank HEPES buffer solution (10 mM, pH 8.0). Scan rate: 100 mV/s.

redox wave at $E_{1/2} = 0.165$ V (vs Ag−AgCl) is observed, demonstrating successful immobilization of the ferrocenyl labeled aptamer on the gold surface.

The redox process of the surface-attached ferrocene group could be represented as[32]

$$\text{-Fc} + X_s^- \rightarrow \text{-Fc}^+X^- + e^- + \text{solv}$$

where -Fc and -Fc^+ are the neutral and oxidized states of the ferrocene group, respectively; X_s^- is the solvated anion in solution; -Fc^+ X^- is an ion pair between the ferrocenium cation and the anion; and solv represents a solvent molecule. The electron and anion should be transferred between the ferrocene moiety and the electrode and between the electrolyte solution and the ferrocene moiety, respectively, upon the redox reaction of the ferrocene group.

A close examination of the shape of the cyclic voltammogram reveals the following characteristics: a broader peak width at half-maximum (fwhm = 146 mV), ideally 90.6/*n* mV, and a greater peak-to-peak separation ($\Delta E_p = 81$ mV) than the ideal of $\Delta E_p = 0$ mV. One possible reason for this peak broadening and the peak-to-peak separation is the slow kinetics for the charge transfer, including the electron transfer between the Au electrode and the Fc moiety and the transport of the anion between the electrolyte and the Fc moiety, through the modified layer. The plots of current density (anodic and cathodic) against the sweep rate are linear, which confirm the existence of a surface-confined Faradaic reaction. The anodic−cathodic peak ratio is close to unity even for slow scan rates. The peak potential shifted only slightly with scan rate up to 200 mV s^{-1}. Thus, the charge transfer is indeed fast, excluding slow electron transfer as a reason for peak broadening and the peak-to-peak separation. Several other factors, including lateral interactions between electroactive groups,[33−37] spatial distribution of redox centers,[38] nonequivalent electroactive sites,[39,40] availability of counterions,[41,42] heterogeneities in the monolayer film,[43] and potential drop effects, have also been proposed to affect the ideality of the redox response.[44]

Alternatively, each Fc head needs to reach the electrode surface to transfer an electron. Therefore, the resulting current may be kinetically controlled by the flexibility of the aptamer chain. Due to the elasticity of the aptamer strands, this may conform to a model of diffusionlike displacement of the ferrocene probe, driven by a concentration gradient within the film, counterbalanced by the "springlike" elasticity of the terminally attached flexible polymeric chain to bring the Fc label in close proximity to the underlying electrode,[45] where the electron could be transferred by tunneling between the ferrocene group and the gold electrode.

In this study, we could suggest that the attached Fc redox moieties do exist in a range of environments with a range of $E°$ values. This is conceivable, in view of the random distribution of the aptamer chains as random coils immobilized with ferrocene at different distances from the electrode surface. This confirms the importance of the orientation of the chain at the surface in determining the voltammetric behavior. The mechanical stresses developed during the oxidation and reduction cycles

(32) Uosaki, K.; Sato, Y.; Kita, H. *Langmuir* **1991**, *7*, 1510−1514.
(33) Laviron, E. *J. Electroanal. Chem.* **1974**, *52*, 395−393.
(34) Angerstein-Kozlowska, H.; Klinger, J.; Conway, B. E. *J. Electroanal. Chem.* **1977**, *75*, 45−60.
(35) Brown, A. P.; Anson, F. C. *Anal. Chem.* **1977**, *49*, 1589−1595.
(36) Smith, D. F.; Willman, K.; Kuo, K.; Murray, R. W. *J. Electroanal. Chem.* **1979**, *95*, 217−227.
(37) Matsuda, H.; Aoki, K.; Tokuda, K. *J. Electroanal. Chem.* **1987**, *217*, 15−32.
(38) Laviron, E.; Roullier, L.; Degrand, C. *J. Electroanal. Chem.* **1980**, *112*, 11−23.
(39) Peerce, P. J.; Bard, A. J. *J. Electroanal. Chem.* **1980**, *114*, 89−115.
(40) Albery, W. J.; Boutelle, M. G.; Colby, P. J.; Hillman, A. R. *J. Electroanal. Chem.* **1982**, *133*, 135−145.
(41) Ohtani, M.; Kuwabata, S.; Yoneyama, H. *Anal. Chem.* **1997**, *69*, 1045−1053.
(42) Andreu, R.; Calvente, J. J.; Fawcett, W. R.; Molero, M. *J. Phys. Chem. B* **1997**, *101*, 2884−2894.
(43) Benitez, G.; Vericat, C.; Tanco, S.; Lenicov, F. R.; Castez, M. F.; Vela, M. E.; Salvarezza, R. C. *Langmuir* **2004**, *20*, 5030−5037.
(44) Ohtani, M.; Kuwabata, S.; Yoneyama, H. *Anal. Chem.* **1997**, *69*, 1045−1053.
(45) Anne, A.; Bouchardon, A.; Moiroux, J. *J. Am. Chem. Soc.* **2003**, *125*, 1112−1113.

could also lead to a distribution of apparent formal potentials.[46] In addition, the repulsive interaction between the positively charged gold electrode and the positively charged ferrocenium (Fc^+) causes the peaks to become broader. There is also a possibility of the ferrocene moieties interacting with each other. The electron-transfer processes of immobilized redox groups on electrodes are coupled to the rates of transport of the charge-compensating counterions in to and out of the monolayer. In this system, the transport of anionic counterions for the ferrocene/ferrocenium redox couple may be hindered by the largely anionic environment near the electrode.

Integration of the area under either the anodic or the cathodic peak, corrected from the background current, measured at a slow potential scan rate, gives the Faradaic charge required for the full oxidation (or full reduction) of the immobilized layer (Q). The total amount of bound Fc on the electrode surface Γ on the electrode can be calculated quantitatively from $\Gamma = Q/nFA$, where n is the number of electrons transferred ($n = 1$), F the Faraday constant (coulombs per equivalent), and A is the effective surface area (square centimeters), thus yielding $\Gamma = (4.6-3.7) \times 10^{-11}$ mol/cm^2 per effective area in end-bound TBA-Fc chains, which is equivalent to surface density of $\approx 2.25 \times 10^{13}$ strands/cm^2, consistent with the value reported for probes shorter than 24 nucleotides,[47] but much higher than that reported for 3′-Fc(dT)20 oligonucleotide end-tethered to gold electrode surfaces.[45] The difference could be attributed to the hexamethylene linker group, which enhances the oligonucleotide immobilization.[47] Additionally, an improved sensitivity and stability of the biosensor could be achieved using thiolation linkers.[48]

A further understanding of the probe assembly could be gained by immobilization of a ferrocene-free aptamer monolayer, and the electron transfer through the monolayer from 20 mM $[Fe(CN)_6]^{3-/4-}$ couples in HEPES buffer solution of pH 8.0 to the electrode surface is evaluated as a measure of the conductivity of the molecular assembly. The bare gold shows the reduction and oxidation peaks that are typical for a diffusion-limited one-electron redox process. The TBA-Au electrode exhibits a much-reduced signal with a large peak-to-peak separation (E_p). Thus, the electronic communication between the solution electrophore and the gold surface is effectively suppressed, indicating blocking of the gold surface by the TBA. In the present work, the coverage is more likely to correspond to a moderate-density tethered aptamer system.

3.3. Differential Pulse Voltammetry. To further support the choice of counterion, differential pulse voltammograms were recorded after the Fc-TBA-functionalized electrode was exposed to either a 25 mM solution of KCl, LiCl, or NaCl or 20 nM thrombin. All the pH values were adjusted to pH 8.0 with a solution of HEPES buffer. Figure 3 shows a chart diagram for the anodic current signal obtained from these solutions. It is obvious that the current signals are strongly affected by the cations and the current signal increases in the following order: $K^+ > Li^+ > Na^+$. For this reason all further electrochemical experiments were carried out in HEPES buffer only, in the absence of any counterion.

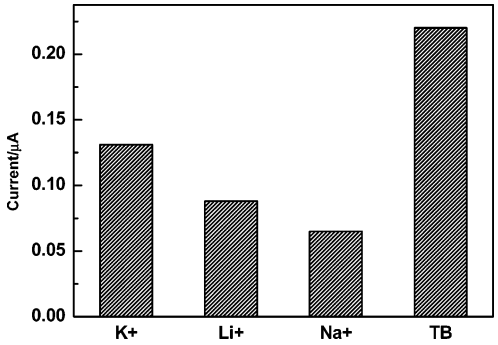

Figure 3. Bar chart of DPV signals for the Fc-TBA-functionalized electrode after exposure to KCl, LiCl, and NaCl (25 mM each) and a 20 nM thrombin solution for 10 min in 0.1 mM HEPES buffer, pH 8.0.

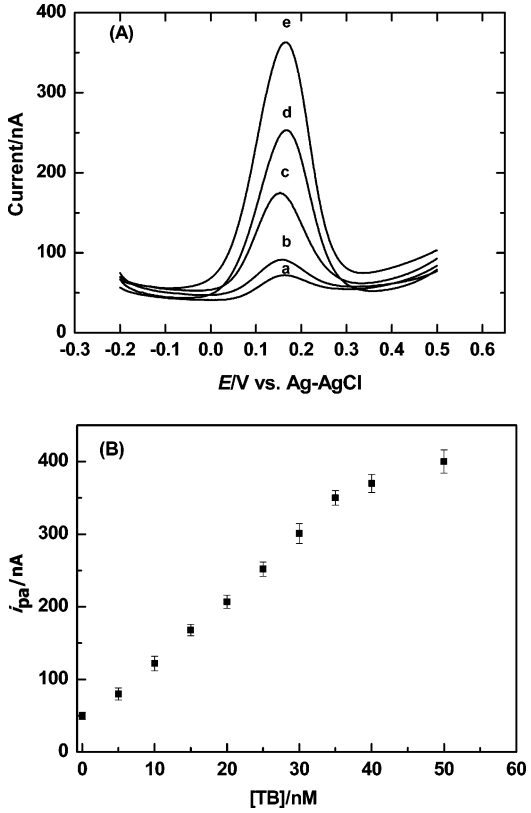

Figure 4. (A) Differential pulse voltammograms (DPVs) in blank HEPES buffer solution (0.01 M, pH 8.0) for (a) Fc-TBA-coated Au electrode, (b) Fc-TBA-2-ME-modified Au electrode (c) after exposure of Fc-TBA-2-ME-modified Au electrode to increasing concentrations of thrombin: (d) 10, (e) 20, and (f) 30 nM thrombin, (modulation amplitude 0.05 V; step potential 0.001 V; scan rate 0.002 V s^{-1}). (B) Calibration plot.

The electrochemical behavior of the immobilized 5′-Fc-TBA-SH-3′ was also investigated by differential pulse voltammetry (DPV). DPV is a pulse technique that allows much higher sensitivity than conventional sweep techniques when detecting very low concentrations of a redox probe. This is achieved by applying a small voltage pulse superimposed on the linear voltage sweep and sampling the differential current at a short time after the pulse. Hence, the measured current is only a product of the Faradaic process, with the capacitive charging current eliminated.[49]

Figure 4 shows typical differential pulse voltammograms (modulation amplitude 0.05 V; step potential 0.001 V; scan rate 0.002 V s^{-1}) for Fc-TBA/Au electrode with a anodic scan in

(46) Posadas, D.; Fonticelli, M.; Rodriguez Presa, M. J.; Florit, M. I. *J. Phys. Chem. B* **2001**, *105*, 2291−2296.
(47) Fan, C.; Plaxco, K. W.; Heeger, A. J. *Proc. Natl. Acad. Sci. U.S.A.* **2003**, *100*, 9134−9137.
(48) Park, I. S.; Kim, N. *Biosens. Bioelectron.* **1998**, *13*, 1091−1097.

Scheme 1. Schematic Representation of Aptamer Conformation on the Electrode Surface before (Coil-like) and after (Quadruplex) Aptamer−Thrombin Association

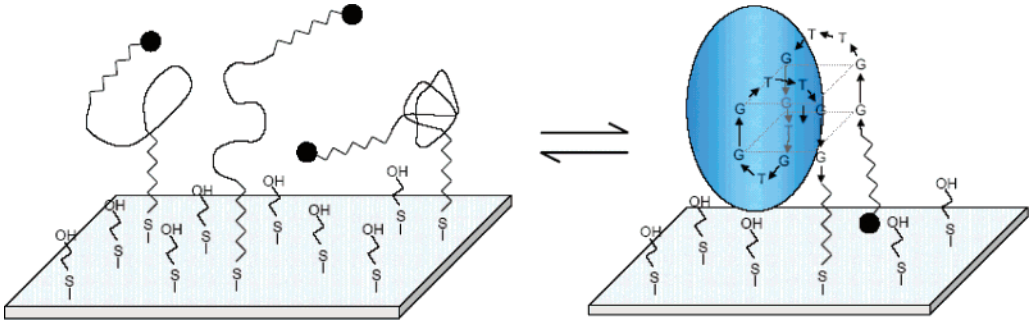

HEPES buffer of pH 8.0 (curve a). The peak of the Fc oxidation current shows increases, after coadsorption of the small blocking agent 2-ME (curve b). The aptamer strand was primarily tethered though a sulfur−gold linkage with the presence of multiple contacts between each strand and the substrate.[50] The nucleotides can presumably adsorb to gold via multiple amines, as amines are known to adsorb weakly to gold surfaces.[51] The thiol group of the assembled 2-ME effectively displaces the weaker adsorption contacts between aptamer nucleotides and the substrates, leaving the probe tethered primarily through the thiol end group (Scheme 1). Such conformation renders the probe to be more accessible to the target molecules. It is more likely that the nonspecific adsorption limits the flexibility of the chains and consequently hinders the diffusion of the redox probe toward the electrode surface. Moreover, the displacement of nonspecific adsorption provides free volume into the film, which enhances the counteranions and solvent transport through the modified film. It is worth mentioning that the surface coverage by the 2-ME prevents the nonspecific adsorption of thrombin on the electrode surface.

The anodic current signal increases after the addition of thrombin, Figure 4c−e, could be attributed to the conformation changes, which will shift the equilibrium toward the quadruplex structure, leading to an approach of the redox label to the electrode surface and the signal transduction is significantly enhanced between a linked label and the gold surface. The signal shows a slight shift to more anodic values, probably due to local medium effects on redox-active moiety. Polynucleotide strand conformations have previously been suggested to account for the electroactivity changes of an electroactive group tethered to a probe strand or a target strand.[52,53]

As shown in Figure 4B, the anodic current signal increased for increasing concentration of thrombin dropped onto the electrode surface. The Fc oxidation signal shows a linear response with the thrombin concentration in the range 5.0−35.0 nM with a correlation coefficient of $r = 0.9988$. When the thrombin concentration was increased to 40 nM and more, the ferrocene signal began to level off, suggesting that most of the Fc-aptamer probes have been associated with the thrombin target. The plot of i_{pa} against the target concentration with relatively small error bars (RSD ranging from 3.8% to 10.0%) indicates that the method is quite reproducible. The slope of the linear plot is 8.94 nA/nM, and the estimated detection limit (defined as DL $= 3S_B/m$, where m is the slope of the corresponding calibration curve and S_B is the standard deviation of the blank) is 0.5 nM. With respect to clinical application, during the initial phase of coagulation thrombin is produced in nanomolar concentrations; thus the linear range of the aptasensor is clinically relevant.[54,55]

The specificity was further tested with DPVs of the Fc-TBA-Au-functionalized electrode in the presence of three proteins, namely, IgG, BSA, and streptavidin. IgG (molecular mass 150 kDa, p*I* 6.1−8.5) and bovine serum albumin (BSA, molecular mass 66 kDa, p*I* 4.2−5.2) were chosen as representatives of proteins present in blood. Streptavidin is characterized, as thrombin, by a neutral isoelectric point, which may favor unspecific binding, and a molecular mass of 52 kDa (compared to 38 kDa for thrombin). The functionalized electrode was exposed to a solution of 50 μL containing 20 nM protein for 10 min. After it was washed with copious amounts of deionized water, the DPV was measured. No detectable change in anodic signal over that of the functionalized electrode was observed, further confirming the specific nature of the aptamer−thrombin interaction. This also demonstrates that the original specificity is retained even after modification or surface tethering.

3.4. Electrochemical Impedance Spectroscopy. Figure 5 shows the impedance spectra in the form of a Nyquist plot for (a) Fc-TBA-coated Au electrode, (b) Fc-TBA-2-ME-modified Au electrode, and (c) after exposure of Fc-TBA-2-ME-modified Au electrode to 20 nM thrombin at the formal potential in HEPES buffer of pH = 8.0. The impedance data are analyzed on the basis of the Vorotyntsev theoretical model of a surface-confined redox system[56] that takes into account the charge-transfer process at the film/electrolyte interface as well as charge diffusion through the film. The impedance data were fitted to an equivalent electronic circuit, shown as an inset in Figure 5, which includes the electrolyte resistance, R_e; electrolyte/film interface $R_{e/f}$; film resistance, R_f; electrolyte/film interface capacity, $C_{e/f}$ (used as a constant phase element, CPE, to improve the fitting of the experimental data); film capacity, C_f; and the Warburg impedance, Z_W, resulting from diffusion of the redox probe. Similarly, this equivalent circuit has been recently

(49) Steel, A. B.; Levicky, R. L.; Herne, T. M.; Tarlov, M. J. *Biophys. J.* **2000**, *79*, 975−981.
(50) Bard, A. J.; Faulkner, L. R. *Electrochemical Methods: Fundamentals and Applications*; John Wiley & Sons: New York, 1980.
(51) Leff, D. V.; Brandt, L.; Heath, J. R. *Langmuir* **1996**, *12*, 4723−4730.
(52) Levicky, R.; Herne, T. M.; Tarlov, M. J.; Satija, S. K. *J. Am. Chem. Soc.* **1998**, *120*, 9787−9792.
(53) Piro, B.; Haccoun, J.; Pham, M. C.; Tran, L. D.; Rubin, A.; Perrot, H.; Gabrielli, C. *J. Electroanal. Chem.* **2005**, *577*, 155−165.
(54) Butenas, S.; Mann, K. G. *Biochemistry (Moscow)* **2002**, *67*, 3−12 (translated from *Biokhimiya* **2002**, *67*, 5−15).
(55) Spiridonova, V. A.; Kopylov, A. M. *Biochemistry (Moscow)* **2002**, *67*, 850−854 (translated from *Biokhimiya* **2002**, *67*, 706−709).
(56) Vorotyntsev, M. A.; Daikhin; L. I.; Levi, M. D. *J. Electroanal. Chem.* **1994,** *364*, 37−49.

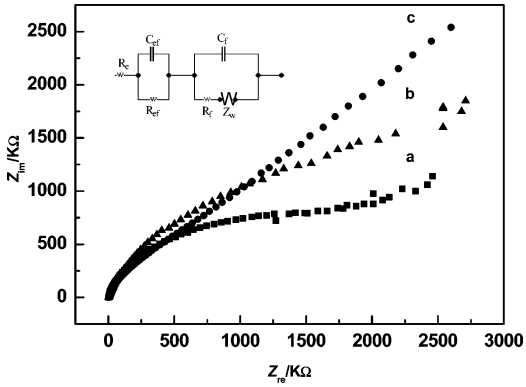

Figure 5. Nyquist plot (Z_{im} vs Z_{re}) in HEPES buffer (0.01 M, pH 8.0) at 0.165 V for (a) Fc-TBA-coated Au electrode, (b) Fc-TBA-2-ME-modified Au electrode (c) after exposure of Fc-TBA-2-ME-modified Au electrode to 20 nM thrombin. Frequency range, 100 mHz−10 kHz; ac amplitude, 5 mV.

Table 1. EIS Results Obtained by Fitting of Experimental Data to Circuit[a]

	R_e, Ω cm^2	$C_{e/f}$, μF cm^{-2}	$R_{e/f}$, Ω cm^2	C_f, μF cm^{-2}	R_f, KΩ cm^2	$W \times 10^{-5}$
Fc-TBA/Au	63	4.75	7180	35	22.4	0.277
Fc-TBA-2-ME /Au	74	4.65	7440	77	33.2	0.221
20 nM thrombin added	62	7.8	10.2	23	6.74	0.115

[a] Shown as an inset in Figure 5.

proposed to interpret the electrochemical behavior of oligonucleotide probe-modified GC electrode.[52]

EIS results obtained by computer fitting of the experimental spectra in Figure 4a−c, using the equivalent circuit shown as an inset in Figure 5, are collected in Table 1. For the sake of simplicity, we basically consider the changes in elements parameters of the Fc-TBA-2-ME-modified Au electrode before and after the association of aptamer with thrombin. Practically, no significant difference was found in the solution resistance, R_e. The association of thrombin could be expected to invoke several significant changes in the layer. The first effect is to cause the approach of the redox label to the electrode surface, leading to significant decrease in the electron-transfer resistance at the electrolyte/film interface $R_{e/f}$, in accord with the increased anodic current signal of differential pulse voltammetry. This effect also results in a decrease in the interplate spacing between the electrode surface and the redox active center, reflected as a increase in $C_{e/f}$. The second effect is to increase the film thickness, as the circular molecule of thrombin has a diameter of about 50 Å,[57] and the other one is the enhanced polarizability of the intervening medium with increasing dielectric constant. The increase in film thickness must give a decreased capacitance, while the increase in the apparent dielectric will induce an increase in film capacitance. These two effects therefore cause shifts in opposite directions. Since a net decrease in film capacitance, C_f, is observed, the effect of film thickness could be envisaged to dominate. The fourth effect could, therefore, involve changes in the structural packing of the aptamer layer when thrombin is associated. The increased electron delocalization in the guanine aromatic π system in the quadruplex structure could enhance the conductive properties of the film. This could be the reason for the considerable decrease in the resistance, R_f, of the film. The noticeable decrease in the Warburg impedance suggests that ion species diffuse more easily through the film.

Finally, to prove that the modified electrode has survived after each impedance measurement, we recorded the DPVs and found that only ca. 5% of its original activity has disappeared. Also, after completion of the impedance measurements, the impedance measurements were reconducted on the same electrode, and this resulted in ca. 93% of the electron-transfer resistance value, indicating that the impedance changes are reversible.

3.5. Regeneration of Electrochemical Molecular Aptamer Beacon. The possibility to optimally regenerate an aptamer-coated surface, and thus reuse it without losing binding efficiency, was studied by carrying out a direct ELAA to detect HRP-labeled thrombin captured by immobilized TBA before and after regeneration of the surface with different known regenerating agents including 1.0 and 0.01 M HCl, 10% and 2% SDS, 0.2 M and 0.05 M Na_2CO_3, 2.0 and 0.1 M NaCl, 1.0 and 0.05 M NaOH, 1.0 and 0.01 M LiCl, and 2.0 and 0.01 M glycine. After the regeneration step was performed, absorbance values were very similar for all the regenerating agents tested and the subsequent thrombin−HRP recognition experiment was observed to be best for 1.0 and 2.0 M NaCl.

Control 1 proved that none of the regenerating agents caused an effect on the streptavidin layer. The nonspecific adsorption of thrombin−HRP tested in control 2 showed an average value of 0.04 AU, indicating that the AU obtained after the regeneration step is mainly due to nonspecific adsorption. Finally, in control 3 it was observed that the regenerating agents 1 M HCl, 1 M NaOH, and SDS (2 and 10%) caused a decrease in the HRP activity, and this was compensated for in the results shown.

These results demonstrated that all the regenerating agents tested could fully regenerate the TBA-biotinylated surface while keeping the same binding efficiency. Simply to avoid the use of metal ions, 1.0 M HCl was chosen as the regenerating agent for electrochemical studies. The anodic response observed for the target was diminished after regeneration appreciably and the main voltammetric features were reversed after the process. Reassociation has completely restored the increased anodic peak of the DPV. This behavior clearly indicated the potential for repeated use of the aptasensor. The cycle of capture, release, and analysis repeated ($n = 25$) on the same modified electrode for 20 nM thrombin solution gave a relative standard deviation of 5.4%.

4. Conclusions

In conclusion, we have demonstrated an electrochemical aptasensor for the reagentless detection of a protein target, thrombin. We have described here a novel synthesized ferrocene-attached thrombin-binding aptamer, self-assembled on polycrystalline gold electrode, with a terminus tethered on the electrode surface and the other terminus labeled with ferrocene in a molecular beacon format. The modified electrode system was characterized by CV, DPV, and EIS. A quasi-reversible redox peak corresponding to the redox reaction of the surface-confined Fc moieties was observed. The conformation change from coil-like to quadruplex structure upon association of aptamer with thrombin induces a significant increase in the Fc anodic current peak, thus facilitating a "switch on" detection, while the use of Fc as a label with lower anodic potential is

(57) Weisel, J. W.; Nagaswami, C.; Young, T. A.; Light, D. R. *J. Biol. Chem.* **1996**, *271*, 31485−31490.

advantageous to avoid the disassembly of the SAM. The reported sensor achieves impressive sensitivity and selectivity, with nanomolar detection limits and negligible response to nonspecific proteins being obtained. Attainment of response is extremely rapid, being achievable within minutes by the detection methods employed, and it is believed that even faster detection is achievable via alternative transduction routes (e.g., amperometry). The aptasensor could be easily and rapidly regenerated and could be reused at least 25 times without any discernible loss in activity. The platform described here could be used as a general approach for the electrochemical detection of aptamer−protein target interaction where an aptamer-specific conformational change would result in "switch-on" or "switch-off" of signal upon target binding. Alternatively, the aptamer could be engineered to undergo a specific conformational change due to target binding. Thus, the simple strategy described here may easily be applied to any molecular aptamer beacon, as well as to detection of DNA/mRNA, thus opening a realm of applications in diagnostics and proteomics.

Acknowledgment. This work has been carried out with financial support from the Commission of the European Communities, specific RTD program Quality of Life and Management of Living Resources, Project QLK6-CT-2002-02583, Rapid Stroke Marker Detection via immunosensors utilizing Labeless Electrochemical and Resonant Mass Detection. A.-E.R. is supported by a fellowship from the Ministerio de Educacion, Cultura y Deporte (Spain). E.B. is supported by an RED fellowship from the Generalitat de Catalunya (Spain).

JA053121D